ORIGINAL PAPER

Magmatic evolution of the Cadamosto Seamount, Cape Verde: beyond the spatial extent of EM1

A. K. Barker · V. R. Troll · R. M. Ellam ·
T. H. Hansteen · C. Harris · C. J. Stillman ·
A. Andersson

Abstract The Cadamosto Seamount is an unusual volcanic centre from Cape Verde, characterised by dominantly evolved volcanics, in contrast to the typically mafic volcanic centres at Cape Verde that exhibit only minor volumes of evolved volcanics. The magmatic evolution of Cadamosto Seamount is investigated to quantify the role of magma-crust interaction and thus provide a perspective on evolved end-member volcanism of Cape Verde. The preservation of mantle source signatures by Nd–Pb isotopes despite extensive magmatic differentiation provides new insights into the spatial distribution of mantle heterogeneity in the Cape Verde archipelago. Magmatic differentiation from nephelinite to phonolite involves fractional crystallisation of clinopyroxene, titanite, apatite, biotite and feldspathoids, with extensive feldspathoid accumulation being recorded in some evolved samples. Clinopyroxene crystallisation pressures of 0.38–0.17 GPa for the nephelinites constrain this extensive fractional crystallisation to the oceanic lithosphere, where no crustal assimilants or rafts of subcontinental lithospheric mantle are available. In turn, magma-crust interaction has influenced the Sr, O and S isotopes of the groundmass and late crystallising feldspathoids, which formed at shallow crustal depths reflecting the availability of oceanic sediments and anhydrite precipitated in the ocean crust. The Nd–Pb isotopes have not been affected by these processes of magma-crust interaction and hence preserve the mantle source signature. The Cadamosto Seamount samples have high $^{206}Pb/^{204}Pb$ (>19.5), high εNd (+6 to +7) and negative $\Delta 8/4Pb$, showing affinity with the northern Cape Verde islands as opposed to the adjacent southern islands. Hence, the Cadamosto Seamount in the west is located spatially beyond the EM1-like component found further east. This heterogeneity is not encountered in the oceanic lithosphere beneath the Cadamosto Seamount despite greater extents of fractional crystallisation at oceanic lithospheric depths than the islands of Fogo and Santiago. Our data provide new evidence for the complex geometry of the chemically zoned Cape Verde mantle source.

Keywords Ocean Islands · Cape Verde · Stable and radiogenic isotopes · Thermobarometry · Magma-crust interaction

A. K. Barker (✉) · V. R. Troll · A. Andersson
Centre of Experimental Mineralogy, Petrology and
Geochemistry (CEMPEG), Department of Earth Sciences,
Uppsala University, Villavägen 16, 752 36 Uppsala, Sweden
e-mail: Abigali.Barker@geo.uu.se

R. M. Ellam
Scottish Universities Environmental Research Centre (SUERC),
East Kilbride, Scotland, UK

T. H. Hansteen
IFM-GEOMAR, Leibniz-Institute of Marine Sciences,
Wischhofstr. 1-3, 24148 Kiel, Germany

C. Harris
Department of Geological Sciences, University of Cape Town,
13 University Avenue, Upper Campus, Rondebosch, Cape Town
7700, South Africa

C. J. Stillman
Department of Geology, University of Dublin, Trinity College,
Dublin 2, Ireland

Introduction

Ocean Islands are frequently considered as natural laboratories to investigate mantle source heterogeneity with the advantage of the isotopic signatures not being obscured by extensive magmatic differentiation (e.g. Geist et al. 1988; Gerlach et al. 1988; Hoernle et al. 2000; Eisele et al. 2003; Regelous et al. 2003; Thirlwall et al. 2004; Abouchami et al. 2005). Hence, modest attention is given to the geochemical influences of magmatic processes occurring between melting and eruption. This perspective is based on the lack of continental crust underlying Ocean Islands, which is assumed to limit the potential for magma-crust interaction. However, this assumption ignores the influence of the surrounding oceanic lithosphere or crust that would naturally be implicated in the processes of magma evolution. Several studies of ocean islands now argue that processes of magma-crust interaction are more common than typically considered (e.g. O'Hara 1998; Harris et al. 2000; Gurenko et al. 2001; Hansteen and Troll 2003).

This study aims to test the role of fractional crystallisation versus magma-crust interaction during magma differentiation, the depth of magma-crust interaction relative to crystallisation depths and potential sources of contaminants. In addition, we evaluate the preservation of geochemical signatures of the mantle source during magmatic differentiation to reveal information on likely source heterogeneity.

In order to address these issues of magmatic differentiation at Ocean Islands, we turn to the Cape Verde oceanic plateau. The Cape Verde oceanic plateau has a few evolved volcanic centres, specifically the Cadamosto Seamount and the Island of Brava (Fig. 1). These evolved centres are expected to provide the most sensitive records of fractionation and magma-crust interaction, simply due to their higher degree of magma differentiation.

Geological setting

The Cape Verde Rise hosts an archipelago of nine volcanic islands, multiple islets and frequent seamounts, located approximately 500 km west of Senegal, Africa. The Cape Verde Rise is a submarine volcanic plateau with an elevation of 2 km above the 130–150 Ma ocean crust (Crough 1978; Ali et al. 2003). The oldest and most eroded islands occur in the east, whereas the youngest and most volcanically active islands occur in the west, as is the case for the Canary Islands (e.g. Carracedo et al. 1998), but volcanism is focused in two distinct island chains namely the northern and southern islands (Fig. 1; Gerlach et al. 1988). The Cape Verde Rise is associated with an oceanic swell, anomalous heat flow, a geoid anomaly and a seismic tomography anomaly extending into the lower mantle, characteristic of a mantle plume (Courtney and White 1986; Ali et al. 2003; Montelli et al. 2004; Pim et al. 2008). The Cadamosto Seamount is located west of the island of Brava, at the western end of the southern island chain, and is the most seismically active seamount in the Cape Verde area (Fig. 1; Grevemeyer et al. 2010). The Cadamosto Seamount, named after Alvise Cadamosto who is credited with the discovery of the Cape Verde islands in 1456, was sampled by dredging in 1985 during an RRS Charles Darwin expedition to Cape Verde (Hill 1985).

The volcanic islands and seamounts of Cape Verde are dominantly mafic with minor felsic volcanism (Gerlach et al. 1988; Davies et al. 1989; Doucelance et al. 2003; Kokfelt et al. 1998; Holm et al. 2006; Millet et al. 2008; Martins et al. 2009; Dyhr and Holm 2010). The Cape Verde volcanic rocks are typically highly alkaline, being basanitic to nephelinitic in nature (Gerlach et al. 1988; Davies et al. 1989). Volcanic rocks from a wide compositional spectrum, for example MgO from 0 to 20 wt%, have been sampled from Santo Antão and Boa Vista (Holm et al. 2006; Dyhr and Holm 2010). The two exceptions to

Fig. 1 **a** Location map of the Cape Verde Rise, 500 km West of Africa and **b** map of the Cape Verde Rise showing the Cape Verde islands and submarine seamounts. The Cadamosto Seamount, located in the southwest of the archipelago, is marked by a star. Note the two island chains, the northern islands; São Nicolau, São Vicente, Santo Antão and the southern islands; Maio, Santiago, Fogo and Brava. Sodade Seamount in the northwest was discovered during the RV Meteor cruise M80/3 in 2010
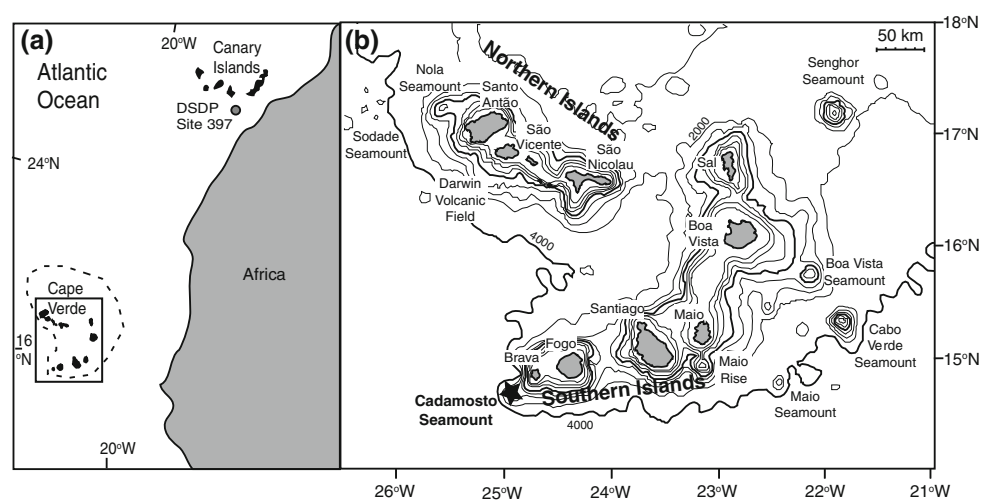
mafic-dominated magmatism at Cape Verde are the island of Brava and the adjacent Cadamosto Seamount. All samples dredged so far from the Cadamosto Seamount are felsic (including two more recent expeditions; pers comm. Hansteen 2010). The island of Brava has a lower submarine unit of nephelinitic composition, a middle alkaline-carbonatite intrusive complex and an upper volcanic unit dominated by phonolites (85%; Madeira et al. 2010). As such, this southwest corner of the Cape Verde archipelago poses questions pertaining to magmatic evolution in general, the relationship between Brava and the Cadamosto Seamount and the reasons for the contrasting composition relative to the rest of the archipelago.

The northern and southern islands display distinct compositions associated with archipelago-scale isotope heterogeneity (Gerlach et al. 1988). The northern islands have high $^{206}Pb/^{204}Pb$ (>19.5), negative $\Delta 8/4$ (Hart 1984), $^{87}Sr/^{86}Sr < 0.7033$ and $\varepsilon Nd > +3$, resulting from mixing between local DMM and young-HIMU or FOZO components (Gerlach et al. 1988; Doucelance et al. 2003; Holm et al. 2006). In contrast, the southern islands display lower $^{206}Pb/^{204}Pb$, positive $\Delta 8/4$, higher $^{87}Sr/^{86}Sr$ and lower εNd (Gerlach et al. 1988; Doucelance et al. 2003; Martins et al. 2009; Barker et al. 2010). The isotope heterogeneity of the southern islands reflects the availability of an EM1-like component in addition to the young-HIMU or FOZO-like component found throughout the archipelago (Gerlach et al. 1988: Doucelance et al. 2003; Martins et al. 2009; Barker et al. 2010). The nature and origin of the EM1-like component are controversial with some authors proposing a component of recycled ocean crust and others arguing for a subcontinental lithospheric mantle source (Hoernle et al. 1991; Kokfelt et al. 1998; Doucelance et al. 2003; Escrig et al. 2005; Abratis et al. 2002; Geldmacher et al. 2008; Martins et al. 2009; Barker et al. 2010). Little or no evidence for crustal assimilation has been recorded in studies of mafic lavas from Cape Verde, probably a consequence of the limited potential for interaction with sediments or crust in the oceanic setting. Although interaction between magmas, oceanic crust and lithosphere has been postulated in the formation of the lavas of São Nicolau (Millet et al. 2008). The few studies that have investigated felsic lavas from the dominantly mafic centres (Santo Antão and Boa Vista) suggest magmatic evolution mainly through processes of fractional crystallisation to generate relatively minor volumes of evolved magma (Holm et al. 2006; Dyhr and Holm 2010).

Analytical methods

Samples were dredged by the RRS Charles Darwin expedition 8/85, dredge number 885/1 sampling at latitude of 14°37.0′, longitude 24°54.0′ and depth 2,500 m (Hill 1985). Weathered edges were removed from samples prior to jaw crushing and milling by agate mortar. Major elements were determined on fused beads by XRF using an automated Philips PW1480 spectrometer at IFM-GEOMAR, Germany. International reference materials BHVO-1, JA-2, JB-2, JB-3 and JR-1 were analysed for calibration, and standards analyses are given in Abratis et al. (2002). Accuracy of standard measurements is <1.2% for SiO_2, TiO_2, Al_2O_3, Fe_2O_3, MnO, and MgO and <6% for CaO, Na_2O, K_2O and P_2O_5; duplicate analyses have reproducibility of <0.15 wt% (2 s.d.) for all oxides. Volatiles (H_2O and CO_2) were analysed upon ignition of powders at 1,200°C using a Rosemount CWA 5003 infrared photometer, and duplicate analyses demonstrate reproducibility of $\leq 0.03\%$ H_2O and CO_2 (2 s.d.). Low oxide totals are associated with significant sulphur contents. Trace elements and sulphur were determined by $HF–HNO_3–$ $HCl–H_2O_2$ digestion of whole-rock powders and analysis by ICP-MS at Acme Analytical Laboratories, Canada (http://acmelab.com/). Most elements have reproducibilities of <8% (2 s.d.), <4% and <3% for LILE and U–Th–Pb, respectively.

Pyroxene, feldspar and feldspathoid compositions were measured by a Cameca SX50 electron microprobe at Uppsala University. Pyroxenes and feldspars were measured with standard operation conditions of 20 kV accelerating voltage and 15nA beam current. Sodium-rich feldspathoid phases were measured with a defocused beam, 20 kV and 10nA to limit rapid Na burn-off. Calibration and standardisation were based on international reference materials, with typical reproducibility as a function of element concentration; >10 wt% ± 1–5%; 1–10 wt% ± 5–10%; <1 wt% ± >10% (Andersson 1997).

Whole-rock powders were leached in 8 N HNO_3 for 4 h and digested with $HF–HNO_3–HCl$. Sr was separated by standard cation exchange procedures, followed by anion exchange for Nd separation, and further analytical details are found in Meyer et al. (2009). Samples were loaded on Re filaments for Sr isotope analysis by VG Sector 54–30 multiple collector mass spectrometer at Scottish Universities Environmental Research Centre (SUERC), East Kilbride, Scotland. Strontium isotope ratios were corrected for mass fractionation using exponential law and $^{88}Sr/^{86}Sr = 0.1194$. The NIST SRM987 standard gave $^{87}Sr/^{86}Sr = 0.710252 \pm 18$ (2 s.d., $n = 48$). Nd isotopes were also analysed by VG Sector 54-30R at SUERC, using $^{146}Nd/^{144}Nd$ of 0.7219 to correct for instrumental mass bias. An internal JM standard gave $^{143}Nd/^{144}Nd = 0.511520 \pm 10$ (2 s.d., $n = 4$). Lead was separated by HBr-based anion exchange, subsequently taken up in 5% HNO_3 and doped with 5 ppb of NIST SRM997 Tl prior to analysis by Micromass IsoProbe MC-ICP-MS at SUERC following the methodology of Ellam (2006). Mass bias was corrected assuming an exponential law and $^{205}Tl/^{203}Tl =$

2.3871. NIST981 analyses gave $^{206}Pb/^{204}Pb = 16.942 \pm 7$, $^{207}Pb/^{204}Pb = 15.508 \pm 8$ and $^{208}Pb/^{204}Pb = 36.748 \pm 21$ ($n = 24$).

Oxygen isotopes of feldspathoid separates were analysed by conventional silicate extraction methods using ClF_3 as the reagent, followed by measurement of isotope ratios of the CO_2 gas produced using a DeltaXP dual inlet gas source mass spectrometer, at the University of Cape Town, South Africa (e.g. Venneman and Smith 1990; Fagereng et al. 2008). Individual clinopyroxenes were analysed by laser fluorination employing BrF_5 as the reagent and measured on O_2 gas (Harris and Vogeli 2010). The conventional oxygen isotope analyses were normalised to SRM28 $\delta^{18}O = + 9.64‰$, and analytical uncertainties are $< \pm 0.15‰$. The laser analyses were normalised using a $\delta^{18}O$ value of $+5.38‰$ for the internal MON GT standard. All values are reported in standard delta notation relative to standard mean ocean water (SMOW).

Samples for sulphur analysis were loaded in tin capsules with tungsten oxide and flash combusted at 1,800°C, and released gases were cleaned and purged in a helium carrier gas and analysed in a Vario II elemental analyser at G.G Hatch Isotope Laboratories, University of Ottawa, following the method of Grassineau et al. (2001). Sulphur isotopes were analysed in SO_2 gas by Thermofinnigan DeltaPlus isotope ratio mass spectrometer. Sulphur isotopes are expressed in $\delta^{34}S$ notation relative to CDT. Sulphanilic acid (Elemental Microanalysis standard B2147) was run as an unknown with the samples to assess analytical precision ($\pm 0.2‰$).

Results

Petrography

The samples can be subdivided into three groups based on mineralogy and geochemistry:

1. Clinopyroxene-nephelinites are green porphyritic samples that contain 0.2–1 mm phenocrysts of clinopyroxene, biotite, titanite, nosean, nepheline, sanidine, Fe-oxides, and ±minor melilite. The groundmass is very fine grained to glassy with apatite needles, feldspar, nepheline and clinopyroxene (Fig. 2a).
2. Cream-coloured porphyritic-phonolites have elongated vesicles and contain 0.5–1 mm phenocrysts of nosean, nepheline, sanidine, ±biotite, ±minor leucite, ±minor Fe-oxides, with groundmass composed of nosean and nepheline, interspersed with apatite needles and opaques (Fig. 2b).
3. Nosean-phonolites are low-density, sandy-coloured samples with equigranular textures (0.1 mm) and contain predominantly nosean, with nepheline, minor
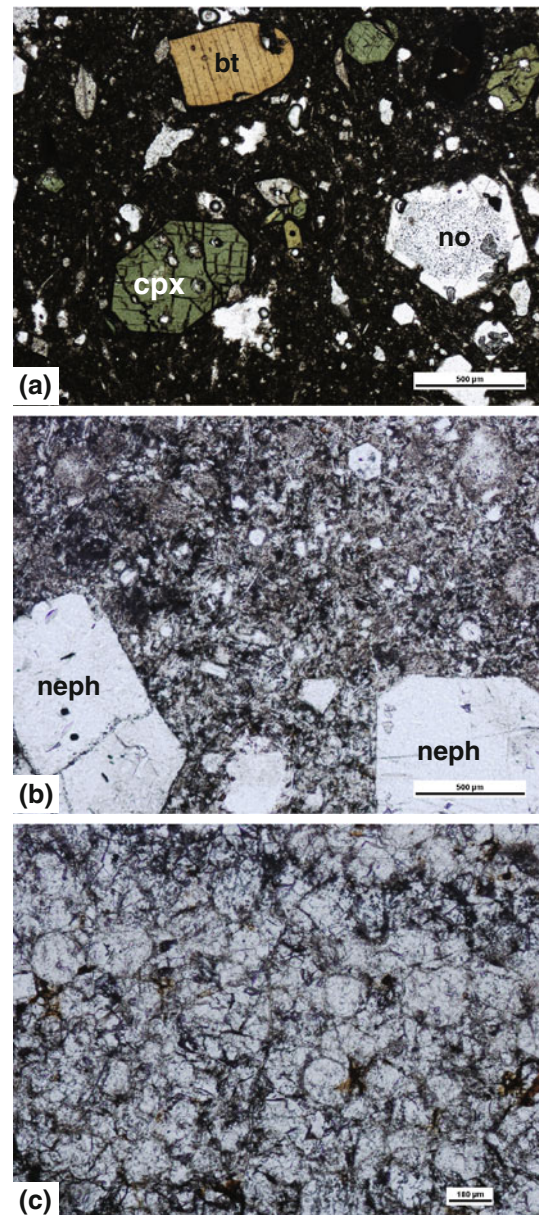
Fig. 2 Photomicrographs of the Cadamosto Seamount lavas **a** clinopyroxene-nephelinites, **b** porphyritic-phonolites and **c** nosean-phonolites. Note the considerably larger phenocrysts in (**a**) and (**b**). Abbreviations for minerals are; *bt* biotite, *cpx* clinopyroxene, *no* nosean, *neph* nepheline

sanidine with occasional microcline, minor biotite, ±Fe-oxides, ±minor leucite, and ±minor titanite (Fig. 2c). Two samples have nepheline and nosean microcrysts in a glassy groundmass.

Sulphur is present as sulphide inclusions in nosean and sulphides in the groundmass. Slight alteration in the Cadamosto Seamount samples by seawater has introduced calcite to vesicles, veins and occasionally patches within the groundmass. Alteration in groundmass has resulted in

patchy clay formation and minor precipitation of iron oxyhydroxides. Such fine-scale features were not possible to eliminate prior to milling and analysis.

Mineral chemistry

Clinopyroxenes have been classified according to Morimoto et al. (1988). The clinopyroxene-nephelinites host Ca–Mg–Fe and Ca–Na pyroxenes, with the latter representing 56% of the clinopyroxenes analysed ($n = 319$). Ca–Mg–Fe pyroxenes are diopside to hedenbergite, and Ca–Na pyroxenes are predominantly aegirine-augite (Fig. 3a, b).

All samples contain feldpathoids, which have been classified according to Na, Ca, and K content revealing nepheline and nosean to be the most common with rare occurrence of leucite (Fig. 3c). The nosean in these samples often contains sulphide inclusions implying that sulphide saturation had been reached at the time of nosean crystallisation.

Minor and sporadically occurring feldspar is Na-sanidine to sanidine in composition (Fig. 3d). If present, large phenocrysts (~ 1 mm) show normal zonation of Or content and specifically Ba content (Fig. 4).

Major and trace elements

Samples from the Cadamosto Seamount contain between 0.7 and 1.9 wt% MgO, plotting amongst the most evolved and silica undersaturated samples from the Cape Verde archipelago (Fig. 5; Holm et al. 2006; Dyhr and Holm 2010). The Cadamosto Seamount samples have low TiO_2 (0.5–1.4 wt%) and P_2O_5 (0.1–0.7 wt%), high Na_2O (9.0–13.1 wt%) and K_2O (3.3–7.5 wt%) and high sulphur contents (0.15–0.56%; Fig. 6). The majority of the samples have LOI < 2.5% except the nosean-phonolites, which have high water contents (3.3–4.3%; Table 2 in Electronic Supplementary Material). These samples also have higher Na_2O and lower K_2O than the porphyritic-phonolites.

The concentrations of Sc are very low (<1.2 ppm), and the concentrations of Y (11.5–49.3 ppm), Nb (170–215 ppm) and Ba (930–1,460 ppm) correlate positively with MgO, Ba and Nb also correlate positively with Y, whereas Zr concentrations (900–1,120 ppm) show no correlation with MgO or Y (Fig. 6). The trace element ratios Zr/Nb and Zr/Y are elevated with the most evolved samples having very high Zr/Y ratios. The nephelinites with ~ 1.7 wt% MgO have highly enriched LREE patterns (La/Yb = 22–29). The phonolites have ~ 0.7 wt% MgO,

Fig. 3 Mineral chemistry of the Cadamosto samples, **a** Quadralateral clinopyroxenes, **b** Ca–Na pyroxenes, **c** feldspathoids, and **d** Feldspars
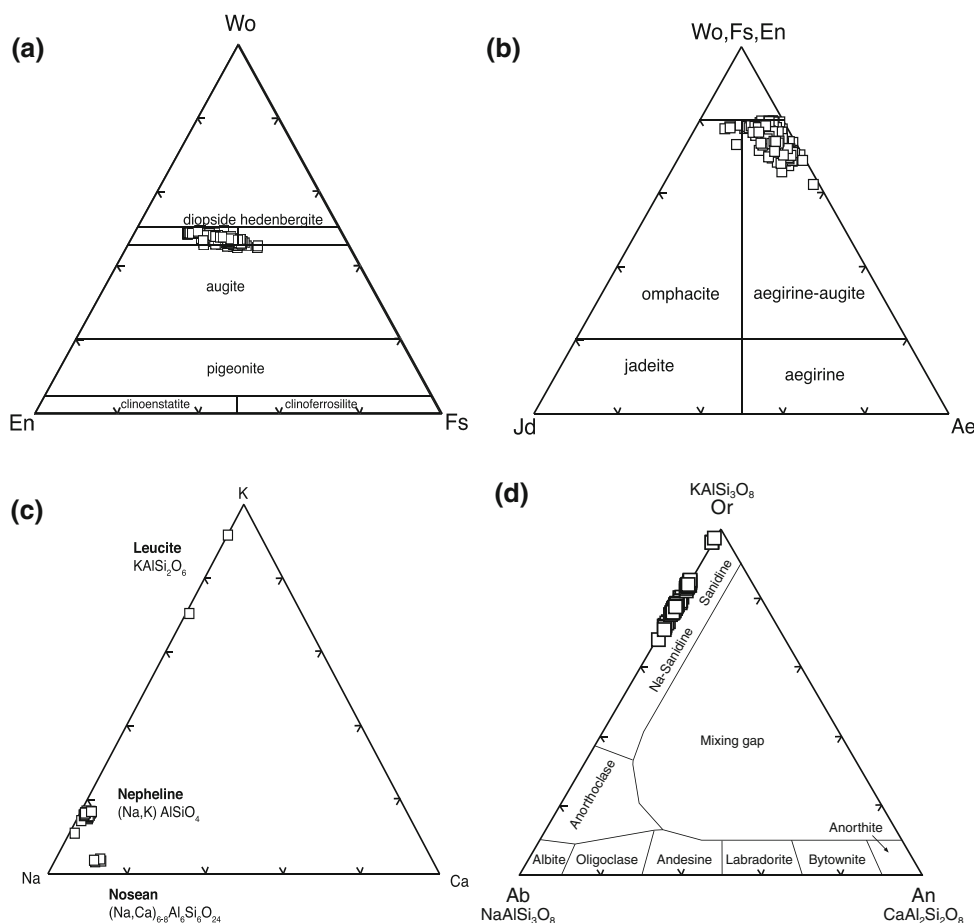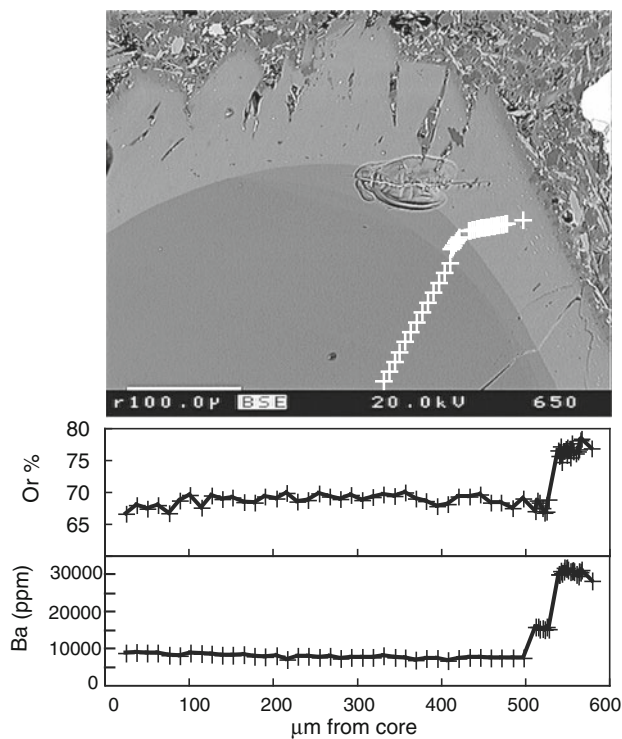
Fig. 4 Zonation of Ba and orthoclase in sanidine from sample D885/1C. The simple rim zonation is shown by orthoclase content, whereas multiple zones are apparent in BSE imaging and Ba content

but are less enriched in LREE (La/Yb = 9–14), and relatively depleted in MREE (Fig. 7). In addition, V, Co and REE decrease with decreasing MgO, and copper concentrations are very low (1.7–12.5 ppm). Total sulphur contents are ~0.5% in the clinopyroxene-nephelinites and 0.15–0.2% in the porphyritic- and nosean-phonolites (Fig. 6), which correlate with $Fe_2O_3^{total}$, Zn and Co, but not with Cu or Ni.

Elements that are susceptible to alteration show varied behaviour; Cs scatters in all sample groups, Ba concentrations are high in the nephelinites and lower in the phonolites, whereas the phonolites have higher Li concentrations, and one nosean-phonolite shows even higher Li (Fig. 8). Rubidium concentrations are constant over the range in MgO in the clinopyroxene-nephelinites to porphyritic-phonolites, whereas the nosean-phonolites cluster at lower Rb, with two samples showing scatter to higher Rb.

Stable and radiogenic isotopes

The Cadamosto Seamount samples have $\delta^{18}O$ of +6.3 to +7.1‰ for feldspathoid separates, with no apparent differences between sample types. Generally, samples with elevated $\delta^{18}O$ (+6.4 to +6.6‰) have higher SiO_2 and $^{87}Sr/^{86}Sr$, than the clinopyroxene-nephelinite with

$\delta^{18}O = +6.3$ and a few samples plot to higher $\delta^{18}O$ of ~+7‰ at variable SiO_2 (Fig. 9). The expected fractionation between nepheline and magma (ΔNe-Magma) at equilibrium is +0.55‰ (at 1,050°C; Zhao and Zheng 2003, their Table 8); hence, nepheline crystallising from a nephelinite melt with $\delta^{18}O$ of +5.7 ± 0.3‰ would have a $\delta^{18}O$ of +6.25‰, similar to the lowest $\delta^{18}O$ of +6.3 ± 0.1‰ in the Cadamosto Seamount samples. Clinopyroxene-melt fractionation (ΔDi-Magma; Zhao and Zheng 2003) of −0.16‰ from a mantle source with $\delta^{18}O$ of +5.7 ± 0.3‰ (Ito et al. 1987) predicts clinopyroxenes with $\delta^{18}O$ of +5.54 ± 0.3‰ at equilibrium. Hence, the clinopyroxenes from the Cadamosto Seamount with $\delta^{18}O$ of +5.3‰ are consistent with expected fractionation from a mantle melt.

The Cadamosto Seamount samples have elevated $\delta^{34}S$ of +4.7 to +5.9‰. The more evolved phonolites, with lower sulphur content, higher SiO_2 and $^{87}Sr/^{86}Sr$ have correspondingly higher $\delta^{34}S$ (Fig. 9).

Alkaline lavas from the Cadamosto Seamount have higher $^{87}Sr/^{87}Sr$ (0.70336–0.70347) at εNd of +6 to +7 than previously sampled in Cape Verde (Fig. 10). The range of $^{87}Sr/^{87}Sr$ occurs over constant εNd. The nosean-phonolites have higher $^{87}Sr/^{87}Sr$ (0.70341–0.70347) than the clinopyroxene-nephelinites and porphyritic-phonolites (0.70336–0.70343).

The Cadamosto Seamount samples have $^{206}Pb/^{204}Pb$ of 19.5–19.8 with negative $\Delta 8/4$ and εNd of +6 to +7 (Fig. 10). Compositional differences between the clinopyroxene-nephelinites, porphyritic-phonolites and nosean-phonolites are not distinguishable in Nd–Pb isotopes.

Discussion

Petrogenesis of the Cadamosto seamount nephelinites and phonolites

We consider the fractionating mineral assemblages and the respective geochemical signatures involved in the petrogenesis of the evolved clinopyroxene-nephelinites, porphyritic-phonolites and nosean-phonolites of the Cadamosto Seamount. We then discuss the geochemical differences between the clinopyroxene-nephelinite, porphyritic-phonolite and nosean-phonolite sample groups and the implications for crystallisation processes and the relationship between their origins.

Clinopyroxene crystallisation has been extensive in all samples, and exhausting the magma of Sc. Titanite crystallisation has led to low Y, TiO_2, depleted MREE and high Zr/Nb, Zr/Hf, Zr/Y, Nb/Ta ratios (Figs. 5, 6, 7). The relative order of partition co-efficients is Zr < Nb, Hf < Y for titanite in highly silica-undersaturated systems (Tiepolo

Fig. 5 Major element variations in the Cadamosto Seamount samples. These samples are some of the most evolved compositions found in Cape Verde shown by comparison to lavas from Santo Antão (Holm et al. 2006), which currently provide the most complete range of magmatic differentiation sampled in Cape Verde
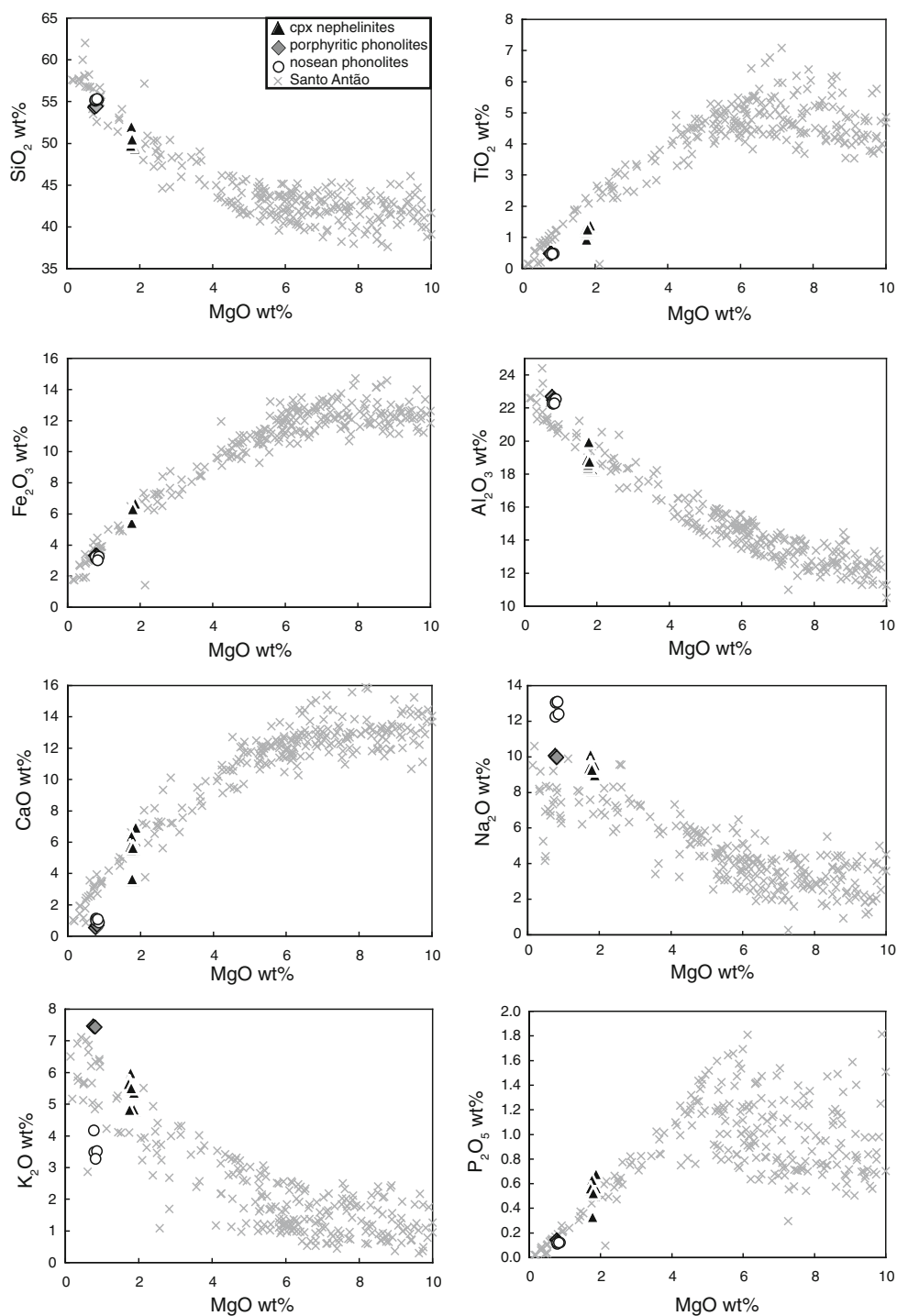
et al. 2002); thus, the relatively constant Zr content allowed high Zr/Nb, Zr/Hf and especially Zr/Y to develop in the magma as titanite crystallised. Additionally, low P_2O_5 is consistent with the presence of apatite in the fractionating assemblage (Fig. 5). The concentrations of V, Co, Fe_2O_3 and TiO_2 decrease with decreasing MgO reflecting crystallisation of Fe–Ti-oxides.

The clinopyroxene-nephelinite to porphyritic-phonolite samples have increasing K_2O, decreasing Ba and constant to slightly increasing Rb with decreasing MgO, suggesting that crystallisation of a K-bearing phase with high partition coefficients for K, Ba and/or Rb such as biotite or amphibole is not important during this stage of differentiation (Weaver 1990; Ewart and Griffin 1994). Instead, the K_2O, Ba, Rb variations

Fig. 6 Selected trace element variations and ratios for the Cadamosto Seamount samples (see text for details). *Grey circles* represent expected fractional crystallisation trend for sulphur (Wallace and Carmichael 1992)
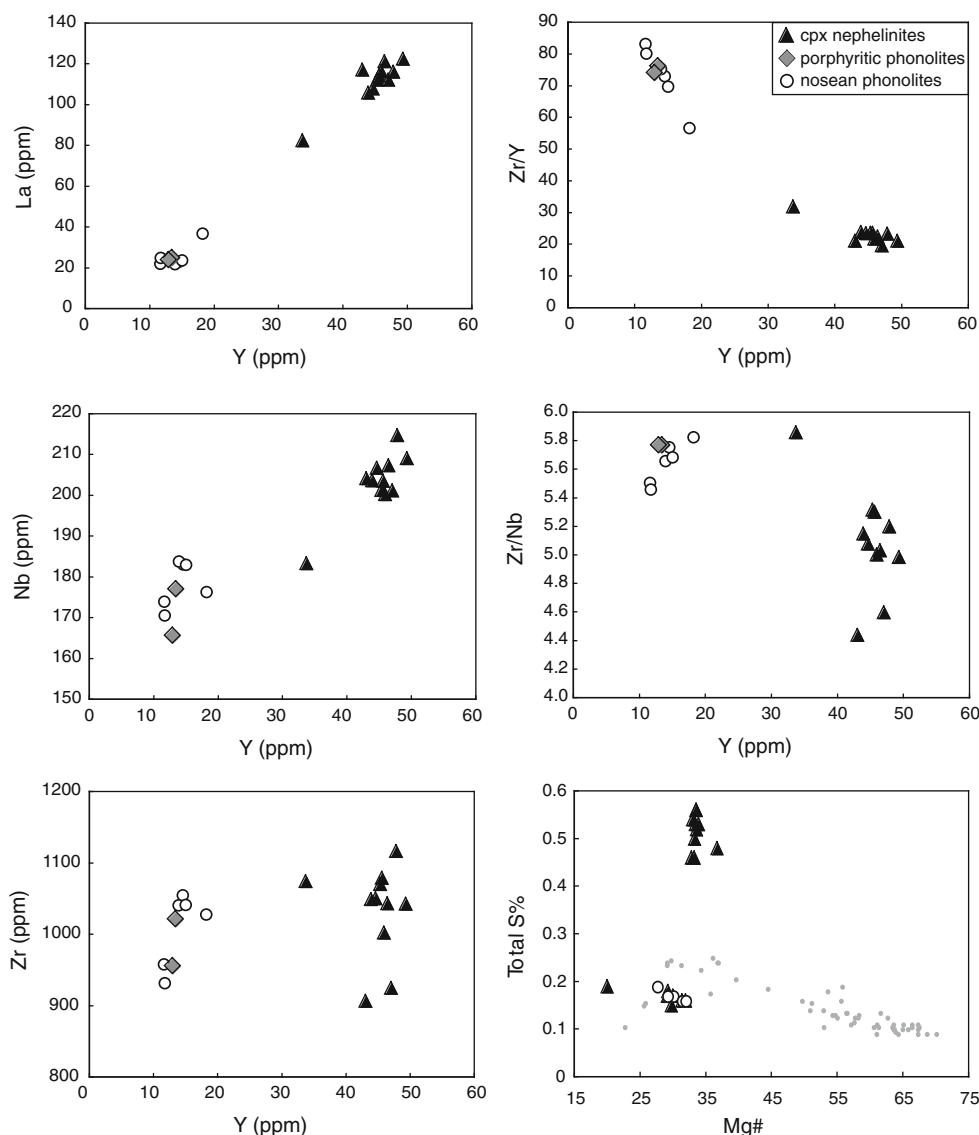
are controlled by crystallisation of titanite, which incorporates Ba, with mildly to moderately incompatible behaviour of K and Rb (Weaver 1990; Ewart and Griffin 1994). The low K_2O content of the nosean-phonolites correlates with low Ba and Rb, suggesting fractional crystallisation of biotite during differentiation. The nosean-phonolites have very high Na_2O (12–13 wt%), associated with high proportions of nosean and nepheline phenocrysts, indicating feldspathoid accumulation (Fig. 5). The sulphur concentrations in the Cadamosto Seamount samples decrease with differentiation along with Fe_2O_3 and Zn concentrations and exhaustion of Cu (Fig. 6), which is consistent with the fractional crystallisation of sulphides and the formation of sulphide inclusions during fractional crystallisation of nosean.

The majority of major and trace elements, therefore, follow liquid lines of descent consistent with fractional crystallisation and removal of clinopyroxene, titanite, Fe–Ti-oxides and apatite. Additionally, the nosean-phonolites

have experienced crystal fractionation and loss of K-bearing phases, but accumulation of Na bearing nosean and nepheline instead. The nosean-phonolites are envisaged to form low-density crystal rafts as crystals concentrate at the top of the magma chamber.

Crystallisation depths in the magmatic plumbing system

Thermobarometric modelling has been employed to determine depths of crystallisation beneath the evolved Cadamosto Seamount. Resulting thermobarometry data constrain the magmatic architecture of the evolved Cadamosto Seamount and allow comparison with nearby mafic volcanic centres of the Cape Verde archipelago.

The clinopyroxene-nephelinites from the Cadamosto Seamount have major element compositions within the calibrated range of the Putirka et al. (2003), Putirka (2008)
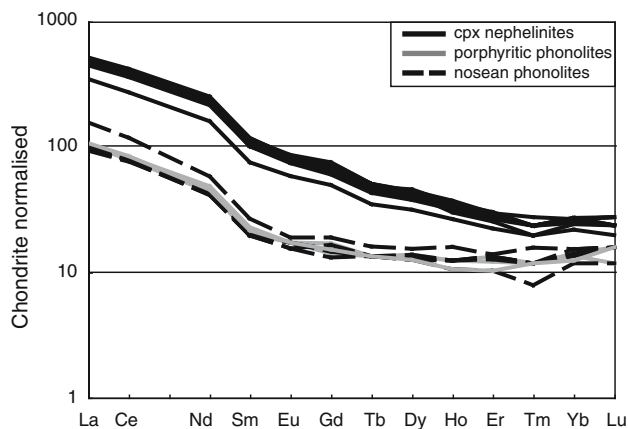
Fig. 7 Rare earth element profiles for the Cadamosto Seamount samples. The porphyritic- and nosean-phonolites have depleted MREE from fractional crystallisation of titanite (see text for discussion)

clinopyroxene-melt thermobarometers, making them suitable thermobarometers. Clinopyroxenes from 7 clinopyroxene-nephelinite samples have been analysed. The Mg# of diopside-hedenbergite and aegirine-augite from these 7 samples span a wide range of Mg# from 40 to 75, with corresponding whole-rock Mg# of 29–37 (Fig. 11). Aegirine-augites generally have lower Mg# than those expected to be in Fe–Mg equilibrium with the melt represented by the whole rock, with only two aegirine-augites falling within equilibrium of $K_D = 0.275 \pm 0.067$ (Fig. 11; Putirka et al. 2003). Correcting the whole rock for

5–10% modal clinopyroxene phenocrysts does not significantly improve the tendency towards equilibrium; thus, calculations are made with only these two equilibrium aegirine-augites. In contrast, the diopside-hedenbergites generally have higher Mg# than the aegirine-augites, and almost 30% of the diopside-hedenbergites are in Fe–Mg equilibrium with the whole rock. Predicted versus observed clinopyroxene components confirm the Fe–Mg equilibrium with standard errors of estimate (SEE) of 0.02 for DiHd, 0.006 for EnFs and 0.02 for Jd (Putirka 2008).

Clinopyroxene-melt thermobarometry on the equilibrium clinopyroxene compositions of the clinopyroxene-nephelinites from the Cadamosto Seamount give crystallisation pressures of 0.45–1.25 GPa (Fig. 11; Putirka et al. 2003; Putirka 2008). The aegirine-augites give the highest pressures for their corresponding nephelinitic samples (1.1 and 1.2 GPa for D885/1C and D885/1E, respectively), although these are within the range of diopside-hedenbergite from other nephelinites. The range in pressure estimates corresponds to depths of 17–46 km, indicating that clinopyroxene crystallisation has dominantly occurred below the 18 ± 1 km Moho (Lodge and Helffrich 2006), and hence within the oceanic lithosphere. These pressures of clinopyroxene crystallisation are similar to clinopyroxene crystallisation pressures of 0.38–0.7 and 0.38–1.1 GPa at the nearby mafic volcanic islands of Fogo and Santiago respectively (Barker et al. 2009; Hildner et al. 2011). This indicates that extensive crystallisation occurs within the oceanic lithosphere beneath Cape Verde.

Fig. 8 Alteration-susceptible trace elements in the Cadamosto Seamount samples (see text for details)
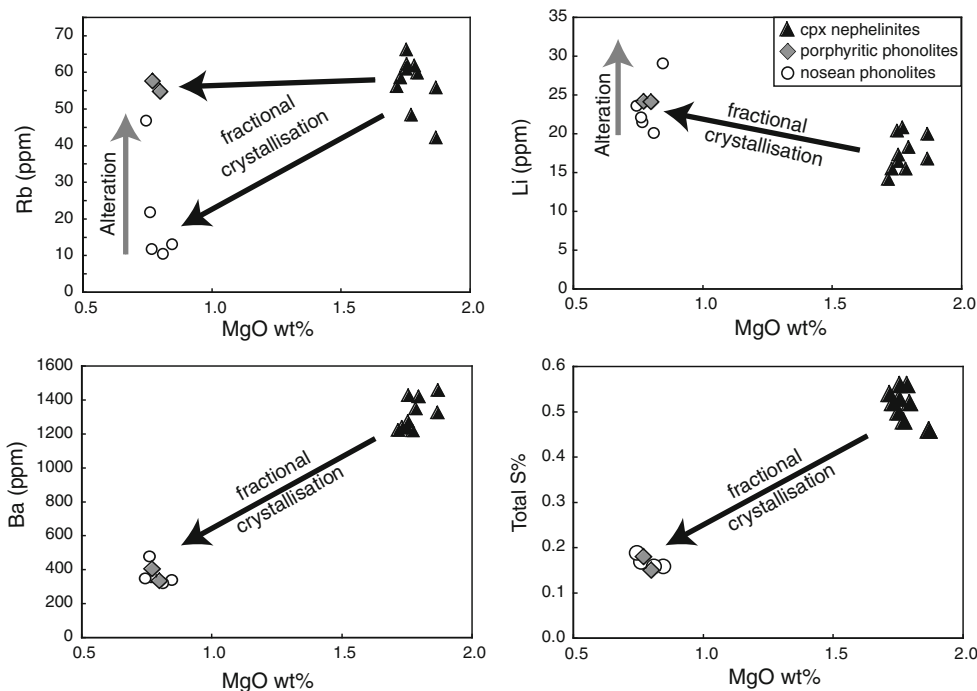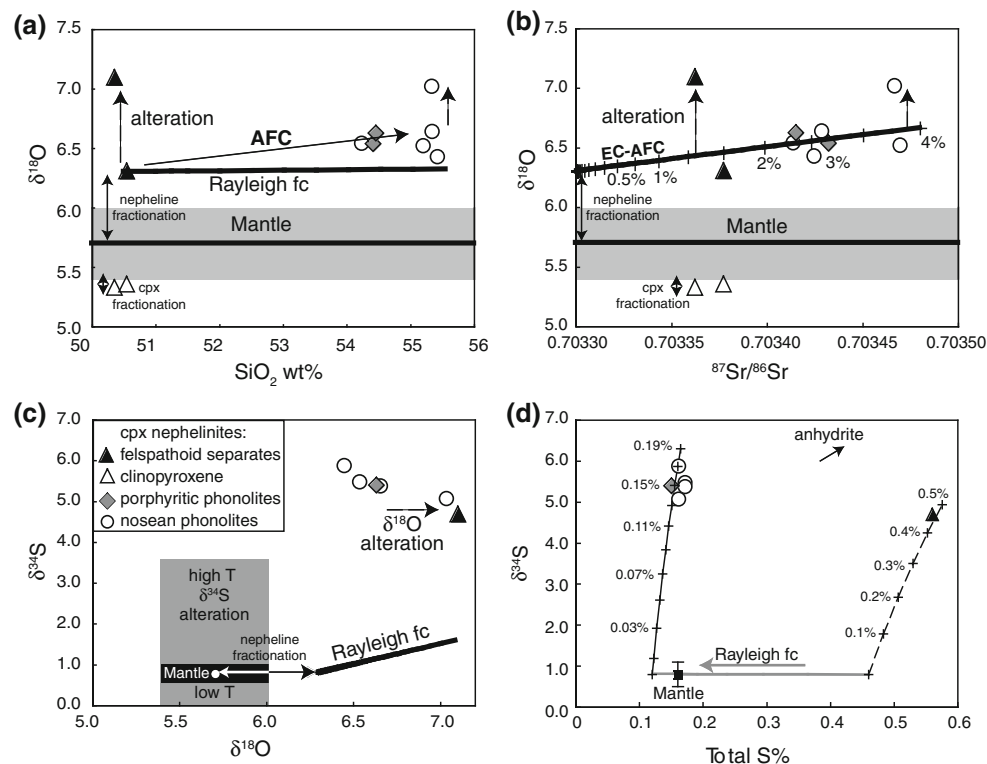
Fig. 9 Stable isotopes of the Cadamosto Seamount samples showing trends for mineral fractionation, Rayleigh fractional crystallisation, seawater alteration, assimilation of sediments and mixing of sediment and anhydrite, **a** oxygen isotopes versus silica, **b** oxygen isotopes versus whole-rock strontium isotopes, **c** whole-rock sulphur isotopes versus oxygen isotopes and **d** sulphur isotopes versus total sulphur content. Analytical uncertainties are within the symbol size. Mantle values refer to $\delta^{18}O$ of $+5.7 \pm 0.3$‰ (Ito et al. 1987) and ocean island mantle from Kilauea with $\delta^{34}S$ of $+0.8 \pm 0.2$‰ (Sakai et al. 1984). Fractionation between nephelinitic melt-clinopyroxene and nephelinitic melt-nepheline was calculated with fractionation factors of $\alpha = 0.99984$ and $\alpha = 1.00055$ respectively (Zhao and Zheng 2003). Rayleigh fractional crystallisation with $\alpha = 0.9998$ for $\delta^{18}O$, consistent with estimates of <1‰ increase in $\delta^{18}O$ with fractional crystallisation (Taylor and Sheppard 1986). Rayleigh fractional crystallisation for $\delta^{34}S$ between nephelinites and phonolites with $\alpha = 0.9980519$, based on 50% sulphide and 50% sulphate in the melt, Δsulphide–sulphate $\approx +7.5$‰ at 1,000–880°C (Sakai et al. 1982, 1984), $Y = 0.5$ and $X = 0.5$ (see

Eq. 5, Sakai et al. 1982). Fractional crystallisation of total sulphur content was based on 1.1% crystallisation determined by least squares minimisation of total sulphur from pyrite crystallisation, and subsequent Rayleigh fractional crystallisation was undertaken with a best fit Kd = 130. EC-AFC modelling for assimilation of sediment was performed with $\delta^{18}O = +18.7$‰, $^{87}Sr/^{86}Sr = 0.709288$ and Sr = 1,200 ppm for the sediment (cf. Spera and Bohrson 2001; Hoernle et al. 1991; Hoernle 1998; Hansteen and Troll 2003; Gurenko et al. 2001; www.seddb.org), and a mantle-derived magma ($\delta^{18}O = +5.7$‰; Ito et al. 1987) with feldspathoid fractionation to $\delta^{18}O = +6.3$‰, and comparable primitive Cape Verde magma with $^{87}Sr/^{86}Sr = 0.7033$ and Sr = 800 ppm (Barker et al. 2009, 2010). The binary mixing model employs ocean island magma with $\delta^{34}S = +0.8$‰ (Sakai et al. 1984), sulphur contents of 0.12 and 0.46 wt% based on results of Rayleigh fractional crystallisation for phonolites and nephelinites, respectively, and anhydrite with $\delta^{34}S = +21$‰ and a sulphur content of 23.5 wt% (Gurenko et al. 2001; Rees et al. 1978). Sulphur isotope alteration by seawater ranges ≤ 3.5‰, observed from DSDP Hole 504B (Alt et al. 1989; Hubberton 1983)

The influence of seawater alteration

The samples from the Cadamosto Seamount erupted into a submarine environment, where they have been subject to continuous contact with seawater. Substantial alteration by seawater has the potential to modify the samples and obscure geochemical characteristics derived from the source or magma-crust interaction during transport through the crust. We discuss petrographic, trace element and isotopic evidence that point to minimal influence of seawater alteration.

The samples are relatively fresh; however, the presence of calcite, clay and iron oxyhydroxides does attest to some

influence of low-temperature seawater alteration. The majority of major and trace elements such as the REE, Nb, Y, sulphur and even Ba, which is fluid mobile and therefore susceptible to alteration (e.g. Donoghue et al. 2008), show undisturbed fractional crystallisation trends (Figs. 6, 8). Considering the alkali elements and other fluid mobile elements that would be expected to highlight the effects of seawater alteration, we find that Li also shows a fractional crystallisation trend. However, a single nosean-phonolite has higher Li probably due to low-temperature seawater alteration (cf. Chan et al. 2002). Influences of seawater alteration are seen in the scatter of Rb in the nosean-phonolites and scattered Cs throughout the sample suite.
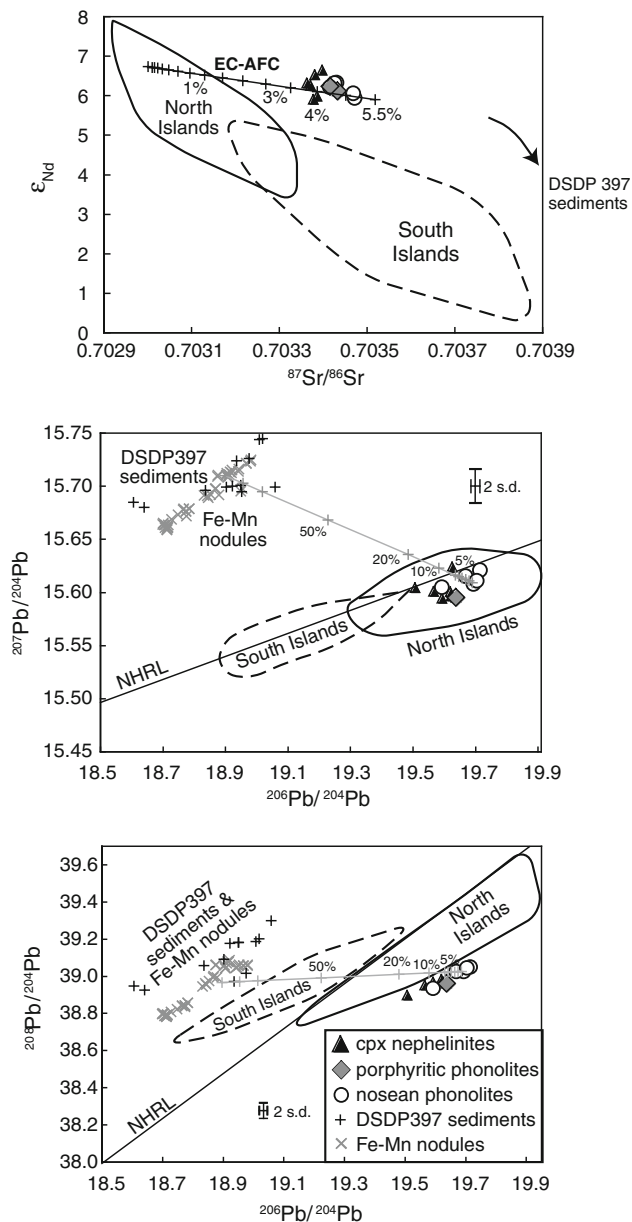
Fig. 10 Radiogenic Sr–Nd–Pb isotopes for the Cadamosto Seamount samples. Fields for northern (*solid black line*) and southern Islands (*dashed line*) from Gerlach et al. (1988), Doucelance et al. (2003), Holm et al. (2006), Barker et al. (2009, 2010). Sediments are from DSDP Hole 397 and Fe–Mn nodules are from the Atlantic (Hoernle et al. 1991; Hoernle 1998; Abouchami et al. 1999). The NHRL is shown for reference (Hart 1984). An EC-AFC model trajectory is shown for assimilation of sediment with $^{87}Sr/^{86}Sr = 0.709288$, $\varepsilon Nd = -7.5$ and $Sr = 1,200$ ppm and $Nd = 16.5$ ppm (Spera and Bohrson 2001; Hoernle et al. 1991; Hoernle 1998), by a primitive Cape Verde magma ($^{87}Sr/^{86}Sr = 0.7030$, $\varepsilon Nd = +6.7$ with $Sr = 800$ ppm and $Nd = 20$ ppm; Barker et al. 2009, 2010). Analytical uncertainties are within the symbol size unless otherwise shown

This illustrates that there is a small variation in alteration-susceptible trace elements, but that most of the trace elements have not been significantly influenced by post-emplacement seawater alteration.

Trace elements that are applicable to the isotopes presented in this study, such as Sm and Nd, show pristine fractional crystallisation trends. Only two clinopyroxene-nephelinites have lower Pb than expected and appear to have lost Pb. However, mobilisation of Pb during seawater alteration serves only to redistribute the primary variations in Pb isotopic signatures of the oceanic crust without providing an additional source of Pb (Pedersen and Furnes 2001). In contrast, the U and to a certain extent Th concentrations have been modified, but the timescales of volcanism of the Cadamosto lavas are likely to be on the order of a few million years, which is insignificant to time-integrated in-growth of Pb isotope ratios from modified U–Th–Pb concentration ratios. The Sr concentrations are mostly within fractional crystallisation trends, with just one nosean-phonolite showing higher Sr. Rubidium, in turn, is probably altered by seawater but will not have had time for radiogenic in-growth to influence the $^{87}Sr/^{86}Sr$ of the samples, because the Rb/Sr ratios are low (<0.06). The Sr isotope ratios of the Cadamosto Seamount samples fall in a tight cluster from $^{87}Sr/^{86}Sr$ of 0.70336–0.70347, with 0.005% standard deviation, which is very unlikely to be associated with expected scatter produced by low-temperature seawater alteration ($^{87}Sr/^{86}Sr = 0.70271$–0.70370; Kawahata et al. 1987). Additionally, these samples have 800–2,900 ppm Sr and would be difficult to alter significantly by small quantities of seawater that contains merely 8 ppm Sr (Von Damm 2000).

Elevated oxygen isotopes occur in samples with high SiO_2 and $^{87}Sr/^{86}Sr$, implying association with magmatic processes. Two samples, however, show higher $\delta^{18}O$ of $\sim +7$‰, which lack high SiO_2 associated with magmatic variations and is likely to be derived from alteration by low-temperature seawater. Sulphur isotopes are uniformly elevated with $\delta^{34}S$ values between +4.7 and +5.9‰, and all samples plot beyond the typical range for alteration in ocean crust and specifically low-temperature alteration that leads to depleted $\delta^{34}S$ (−2 to +3.5‰; Alt et al. 1989; Hubberton 1983; Alt et al. 1993).

Hence, we conclude that Sr–Nd–Pb isotopes and sulphur isotopes have not been significantly influenced by low-temperature seawater alteration and will provide robust tracers of magma-crust interaction or mantle source variations as appropriate. Oxygen isotope data highlight the variable influence of seawater alteration on two samples. The remaining oxygen isotope data appear robust for tracing processes of magma-crust interaction.

Interaction between magma and the crust

We now consider the origin of elevated $\delta^{18}O$, $\delta^{34}S$ and $^{87}Sr/^{86}Sr$ found in the Cadamosto Seamount samples. The relationship with differentiation and potential assimilants
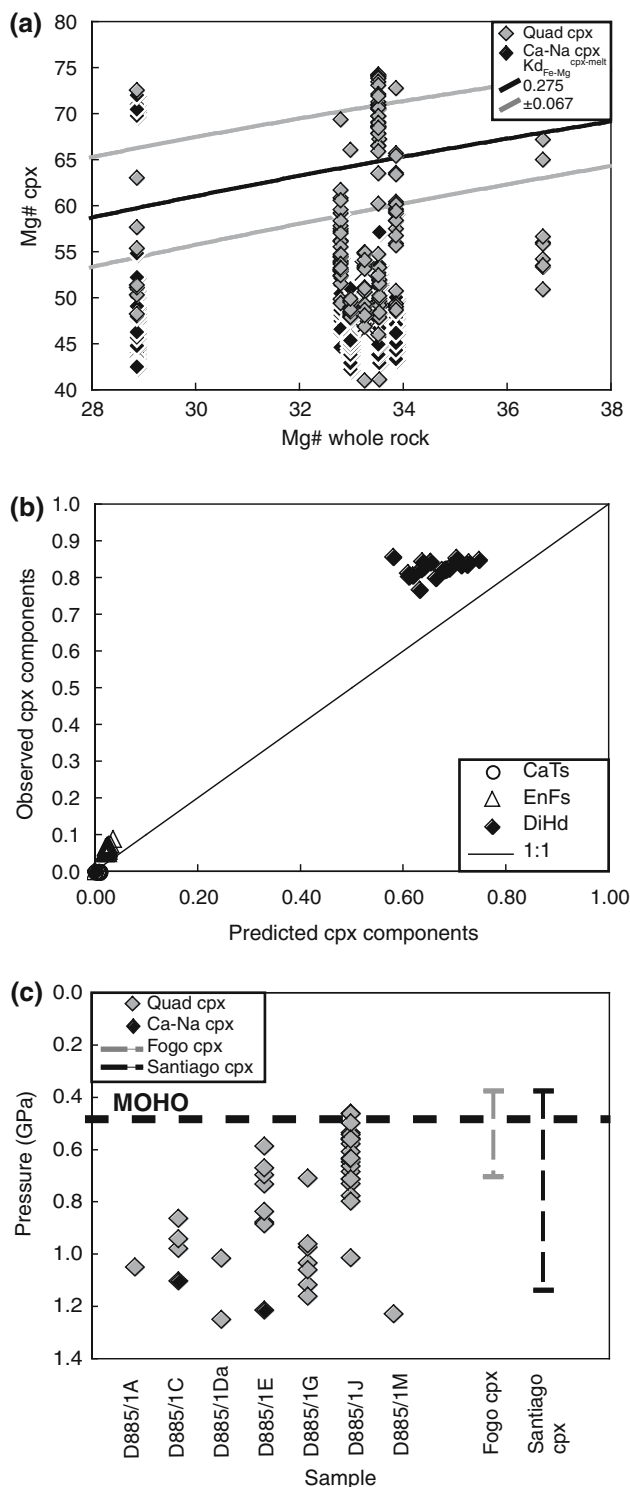
◀ **Fig. 11** Determination of equilibrium between clinopyroxene and melt and clinopyroxene-melt thermobarometry. **a** The Mg# of clinopyroxene versus whole-rock Mg#, in comparison with Kd_{Fe-Mg} between clinopyroxene and melt of 0.275 ± 0.067, *black line* with *grey lines* on either side marking the 1 s.d. uncertainty (Putirka et al. 2003), **b** observed clinopyroxene components from mineral chemistry versus predicted clinopyroxene components from whole-rock composition, **c** results of equilibrium clinopyroxene-melt thermobarometry for quadralateral and Ca–Na pyroxenes from the Cadamosto Seamount compared to nearby islands of Fogo and Santiago (Hildner et al. 2011; Barker et al. 2009). Depths calculated based on a density of 2.8 gcm^{-3} for basaltic oceanic lithosphere. The Moho is shown for reference, from Lodge and Helffrich (2006)

of differentiation. The nosean-phonolites show slightly higher $^{87}Sr/^{86}Sr$ values than the porphyritic-phonolites or clinopyroxene-nephelinites (Fig. 10). The Cadamosto Seamount samples have higher $^{87}Sr/^{86}Sr$ for a given εNd and $^{206}Pb/^{204}Pb$ than previously published data for Cape Verde. The bulk feldspathoid separates generally increase in $\delta^{18}O$ (+6.3 to +6.6‰) from a mantle-like source, whereas clinopyroxenes are consistent with originating directly from a mantle-like source.

The Cadamosto Seamount samples also have higher $\delta^{34}S$ (+4.7 to +5.9‰) than expected for magmas purely derived from an ocean island mantle source (+0.8 ± 0.2‰; Sakai et al. 1984). The processes that have the potential to fractionate and modify the sulphur isotopes are magma degassing, fractional crystallisation or low-temperature seawater alteration. We have modelled the potential influence of these processes to determine the cause of the high $\delta^{34}S$ values (Fig. 12; Hubberton 1983; Ueda and Sakai 1984; Sakai et al. 1982, 1984; Alt et al. 1989, 1993; de Hoog et al. 2001). The high total sulphur concentrations suggest that sulphur was incompatible during fractional crystallisation between the primitive magma and the clinopyroxene-nephelinites (Fig. 6); thus, the $\delta^{34}S_{sulphate-sulphide}$ of the magma would not have fractionated. At some stage, sulphur saturation was reached as is indicated by the growth of sulphide inclusions in nosean. Hence sulphide precipitation from the magma would have fractionated the sulphide-sulphate ratio and therefore the $\delta^{34}S$ of the magma (Alt et al. 1993). We assume that the proportions of sulphide and sulphate in the magma were 50:50 and that $\Delta_{sulphate-sulphide} \approx +7.5\%$ (at 1,000–880°C; Sakai et al. 1982, 1984). Subsequent modelling for Rayleigh fractional crystallisation under such conditions proceeds with a fractionation factor of $\alpha = 0.9980519$ and leads to an increase in $\delta^{34}S$ to ca. +0.81‰ for a 0.3 fraction of sulphur from an ocean island mantle source with $\delta^{34}S$ of +0.8‰, which is much lower than observed in the Cadamosto Seamount samples. Magma degassing is expected to modify $\delta^{34}S$ of magmas during their ascent through the uppermost crust, modelling for degassing of SO_2 with a fractionation factor of $\alpha = 0.998$ suggests that

are investigated through modelling of assimilation processes. Furthermore, crystallisation depths are integrated with Sr–O–S isotopes to infer likely depth and occurrence of magma-crust interaction and the origin of assimilants.

Once the samples have been filtered for seawater alteration, the remaining samples exhibit elevated $\delta^{18}O$, $^{87}Sr/^{86}Sr$, $\delta^{34}S$, SiO_2 and are associated with other indices
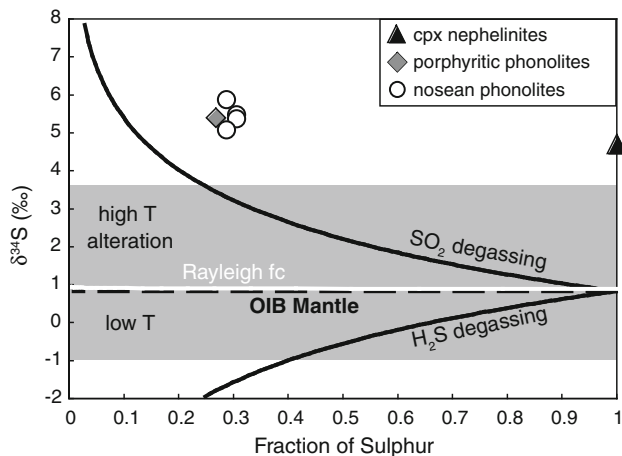
Fig. 12 Sulphur isotope variations of the Cadamosto Seamount in comparison with expected variations due to magma degassing, fractional crystallisation, and seawater alteration. Based on deviations from ocean island mantle from Kilauea ($0.8 \pm 0.2\permil$; Sakai et al. 1984), degassing with fractionation factor H_2S-melt $\alpha = 1.002$ and SO_2-melt $\alpha = 0.998$ (*solid black lines*), and Rayleigh fractional crystallisation with $\alpha = 0.9980519$ (*solid white line*; Sakai et al. 1982, 1984; Alt et al. 1993). The fraction of sulphur is calculated from the sulphur content of the clinopyroxene-nephelinite sample (0.56% total S; see Table 2 in Electronic Supplementary Material). Range of $\delta^{34}S$ of ocean crust from DSDP Hole 504B altered at high and low temperatures (*grey box*; Alt et al. 1989; Hubberton 1983) (see text for details)

this would be expected to perturb the $\delta^{34}S$ of lavas up to ca. $\delta^{34}S$ of $+3.2\permil$ for corresponding sulphur loss, still a good deal lower than the Cadamosto Seamount samples ($\delta^{34}S = +4.7$ to $+5.9\permil$). Low-temperature seawater alteration is likely to deplete the samples in $\delta^{34}S$, with higher temperature alteration modifying the $\delta^{34}S$ of pristine volcanics up to $\delta^{34}S$ of $+3.5\permil$, which is still significantly lower than the $\delta^{34}S$ of $+4.7$ to $+5.9\permil$ observed at the Cadamosto Seamount (Hubberton 1983; Alt et al. 1989, 1993). Therefore, the elevated $\delta^{34}S$ values of the Cadamosto seamount samples are not formed by processes of magma degassing, fractional crystallisation or seawater alteration.

The elevated $\delta^{18}O$, $\delta^{34}S$ and $^{87}Sr/^{86}Sr$ of the Cadamosto Seamount samples relative to the Nd–Pb isotopes suggest that they have been selectively modified by a process influencing the groundmass and feldspathoid phenocrysts, but not the clinopyroxene phenocrysts, that occurred during differentiation of the magma. These geochemical signatures suggest a subtle, late-stage influence of magma-crust interaction. We now consider the assimilants available above the depths of clinopyroxene crystallisation, that is, in the crust not the lithospheric mantle, which are igneous oceanic crust, seawater-derived carbonate sediments and oceanic sediments. A suitable assimilant would have high concentration of Sr but low Nd and Pb, so as not to perturb the Nd–Pb isotope signatures. Oceanic crust would not

contain enough Sr (100 ppm vs. samples with 2,800 ppm; Barker et al. 2008), or high enough $^{87}Sr/^{86}Sr$ even when altered by seawater ($^{87}Sr/^{86}Sr = 0.70271$–$0.70370$; Kawahata et al. 1987), or high enough $\delta^{18}O$ to contaminate the magma to such a degree within reasonable thermal constraints. Seawater-derived sediments such as carbonates are rare in the local DSDP Hole 367, probably due to the shallow CCD relative to the ocean depth (CCD < 3,700 m; e.g. Melguen 1978); furthermore, low $\delta^{18}O$ of carbonates makes them unsuitable assimilants (average marine carbonate = 0‰; www.seddb.org). Instead, we have to look to oceanic sediments to find suitable contaminants: Siliciclastic oceanic sediments have an average $\delta^{18}O$ of $+18.7\permil$ (www.seddb.org), and sediments from DSDP Site 397, south of the Canary Islands, have high Sr concentrations ~1,200 ppm and $^{87}Sr/^{86}Sr$ of 0.723619 (Hoernle et al. 1991; Hoernle 1998). Oceanic sediments offer suitable oxygen and strontium isotope contaminants (cf. Hansteen and Troll 2003). Igneous ocean crust and sediments, however, have low $\delta^{34}S$ and an additional assimilant with high $\delta^{34}S$ is required. Seawater has high $\delta^{34}S$ and precipitates minerals such as anhydrite in ocean crust with high S concentration and $\delta^{34}S$ of $+21\permil$ (Rees et al. 1978), requiring only a little anhydrite assimilation for a significant change in $\delta^{34}S$. We undertook a combined approach of modelling the assimilation process by energy constrained—assimilation and fractional crystallisation (EC-AFC; Spera and Bohrson 2001) and standard mixing models (DePaolo and Wasserburg 1979). The modelling results show that the Cadamosto seamount samples can be modelled with 3.5–4.5 and 1.5–4% assimilation of ocean sediments for Sr and oxygen isotopes, respectively. This suggests a decoupling between the behaviour of Sr and oxygen during the partial melting processes associated with assimilation, probably due to the incompatible trace element nature of Sr in contrast to the role of oxygen in mineral structures. These oceanic sediments have low Nd and Pb concentrations 16.5 and 11 ppm, respectively (Hoernle et al. 1991; Hoernle 1998), compared to the lavas 20 and 8 ppm respectively. Therefore they do not modify the Nd–Pb isotopes beyond the analytical uncertainties (Figs. 9, 10). Sulphur isotopes are consistent with assimilation between 0.13 and 0.5% of anhydrite.

The record of this signature of magma-crust interaction in the feldspathoids and whole rocks, but not the clinopyroxenes, indicates magma-crust interaction at pressures shallower than 0.45 GPa, that is following clinopyroxene crystallisation. The magmas feeding the Cadamosto Seamount must encounter sediments and anhydrite that previously precipitated at >150°C in ocean crust (Shanks et al. 1981), suggesting that the anhydrite is found within warm ocean crust, probably overlain by sediments. This is likely to occur where sediments accumulated on the 130 Ma

ocean crust prior to the Cape Verde magmatism that would have covered those sediments by the 2 km submarine plateau and subsequently built up the islands and seamounts.

Assimilation of oceanic sediments to account for Sr and O isotope variations and anhydrite to account for sulphur isotope variations compares well with a model for oxygen and sulphur isotopes of basalt hosted melt inclusions in clinopyroxenes from Gran Canaria proposed by Gurenko et al. (2001), suggesting that processes of crustal assimilation are more common than conventionally perceived in ocean islands.

Constraining the mantle source

Once the isotope data have been filtered for alteration and crustal assimilation, it becomes clear that the Nd–Pb isotopes provide insights into the mantle source of the Cadamosto Seamount, which is put into the wider context of the Cape Verde archipelago to reveal implications for the overall isotope heterogeneity of the Cape Verdes.

Despite the occurrence of minor low-temperature seawater alteration and significant crustal contamination (<5%) of the Cadamosto Seamount samples, the Nd isotopes remain a homogeneous group and the Pb isotopes follow a well-defined linear trend. This observation, along with low Nd–Pb concentrations of seawater and potential crustal contaminants, limits the potential for significant effects of contamination of the magma observed in the Nd–Pb isotopes. Hence, the Nd–Pb isotope data preserve their mantle source signatures and can be used to reveal important information concerning variations in source heterogeneity in Cape Verde.

The Nd–Pb isotope signatures of the Cadamosto Seamount samples show high $^{206}Pb/^{204}Pb$ of 19.5–19.8 with negative $\Delta 8/4$ and εNd of +6 to +7. This is in contrast to the nearby southern islands of Fogo and Santiago, which have lower $^{206}Pb/^{204}Pb$ of <19.5 with positive $\Delta 8/4$ and εNd of <+5 (Gerlach et al. 1988; Doucelance et al. 2003; Holm et al. 2006; Barker et al. 2009; Martins et al. 2009). Instead, the Cadamosto Seamount shares the isotopic signature with the northern islands rather than the nearby southern islands. Thus, the EM1-like component with positive $\Delta 8/4$ and low εNd, characteristic of the southern islands does not occur in the vicinity of the Cadamosto Seamount (Gerlach et al. 1988; Doucelance et al. 2003; Escrig et al. 2005; Barker et al. 2010; Hildner et al. 2011). This constrains the spatial extent of the EM1-like component within the Cape Verde archipelago to the east of the Cadamosto Seamount for the sampled stratigraphic levels (Fig. 13).

The new isotope data for the Cadamosto Seamount together with the recent data from Brava (Hildner et al.
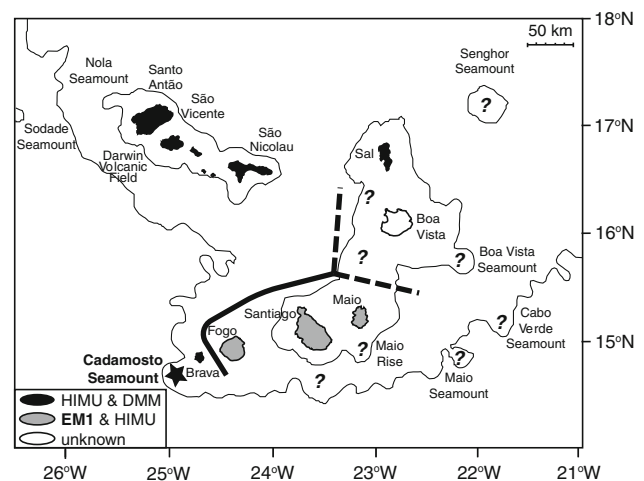
Fig. 13 Map showing the westerly extent of the EM1-like component in the southern island chain of the Cape Verde archipelago. Isotope data used to determine source heterogeneity for individual islands from Gerlach et al. (1988), Davies et al. (1989), Doucelance et al. (2003), Hildner et al. (2011), (see text for details)

2011) allow us to map the spatial extent of the EM1-like component in the southwest of the Cape Verde archipelago (Fig. 13). Re-evaluation of the isotope heterogeneity in the entire Cape Verde archipelago indicates that the southern island chain with positive $\Delta 8/4$ due to the presence of an EM1-like component is defined by Fogo, Santiago and tentatively Maio (based on 2 analyses; Doucelance et al. 2003). Evaluation of the recent isotope data from Brava reported by Hildner et al. (2011) show affinity with the northern islands and the Cadamosto Seamount opposed to the adjacent EM1-like islands by high $^{206}Pb/^{204}Pb$ (19.3–19.9) and negative $\Delta 8/4$. The absence of the EM1-like component indicated by high $^{206}Pb/^{204}Pb$ (>19.5) and negative $\Delta 8/4$ is characterised by the northern islands and the southwestern volcanic centres of Cadamosto and Brava. Mapping the extent of the EM1-like component to the east is more problematic. The older eastern islands share a bathymetric plateau with the southern islands, but uncertainty in the mantle source heterogeneity is introduced by the limited availability of geochemical data, only 3 analyses from Sal (Davies et al. 1989) inferring association with the northern islands and no data from Boa Vista. Hence, the spatial extent of the EM1-like component may extend to include Boa Vista and Sal or have its boundary south of Boa Vista or between Boa Vista and Sal. The EM1-like component is temporally known to exist back to 4.5 Ma (Barker et al. 2010), so there is a chance that the EM1-like component is temporally, opposed to spatially, absent at the time of volcanism on Sal and Boa Vista. Furthermore, the southeastern boundary of the EM1-like component is unknown and requires investigation of the submarine seamounts in this area.

The data presented here show the contrast between crustal assimilation influencing the Sr–O–S isotope systematics and preservation of the mantle source signature in Nd–Pb isotopes allowing the spatial limits of EM1-like component to be constrained. The occurrence of shallow assimilation of sediments and absence of an EM1-like signature in the region of clinopyroxene crystallisation in the oceanic lithosphere strengthen the hypothesis that the EM1-like source lies below the depth of clinopyroxene crystallisation in the oceanic lithosphere, therefore, most likely in the mantle east of the Cadamosto Seamount.

Conclusions

The Cadamosto Seamount has been built up of evolved lavas that have experienced a complicated and dynamic ascent from melting, passage through and storage in the oceanic lithosphere and crust to final submarine eruption, with most of this journey recorded in the lavas. The mantle source has high $^{206}Pb/^{204}Pb$ and εNd for Cape Verde and negative $\Delta 8/4$ similar to the northern islands, indicating that the zone of the EM1-like component stops east of the Cadamosto Seamount. Following melting of the mantle source, magmas have travelled through the oceanic lithosphere where clinopyroxene crystallisation took place. Magmatic differentiation in the oceanic lithosphere modified mafic magmas producing evolved clinopyroxene-nephelinite magmas with 2 wt% MgO, as indicated by clinopyroxene-melt thermobarometry of equilibrium clinopyroxenes (Hildner et al. 2011; Barker et al. 2009). Fractional crystallisation continued during transport of the magmas through the crust, where feldspathoids crystallised and the magmas were contaminated with oceanic sediments and anhydrite precipitated in the old oceanic crust.

The role of assimilation of oceanic sediments and anhydrite from the ocean crust is constrained by modelling of Sr–O–S isotopes to <5 and ≤0.5%, respectively. This probably reflects on the one side the thermal and chemical potential for assimilation by such evolved magmas and on the other a limited timescale of magma storage at levels in the crust where sediments and anhydrite were available for magma-crust interaction.

Establishing the relationship between the Cadamosto Seamount and the adjacent Island of Brava requires investigation of the magmatic evolution of Brava first, in order to provide associated comparisons that will permit exploration of a connection between the two volcanic centres.

References

Abouchami W, Galer SJG, Koschinsky A (1999) Pb and Nd isotopes in NE Atlantic Fe-Mn crusts: Proxies for trace metal paleo-sources and paleocean circulation. Geochimicia et Cosmochimica Acta 63:1489–1505

Abouchami W, Hofmann AW, Galer SJG, Frey FA, Eisele J, Feigenson M (2005) Lead isotopes reveal bilateral asymmetry and vertical discontinuity in the Hawaiian mantle plume. Nature 434:851–856

Abratis M, Schmincke H-U, Hansteen TH (2002) Composition and evolution of submarine volcanic rocks from the central and western Canary Islands. Int J Earth Sci (Geol Rundsch) 91:562–582. doi:10.1007/s00531-002-0286-7

Ali MY, Watts AB, Hill I (2003) A seismic reflection profile study of lithospheric flexure in the vicinity of the Cape Verde Islands. J Geophys Res 108(B5):2239–2263

Alt JC, Anderson TF, Bonnell L (1989) The geochemistry of sulfur in a 1.3 km section of hydrothermally altered oceanic crust, DSDP Hole 504B. Geochim Cosmochim Acta 53:1011–1023

Alt JC, Shanks WC III, Jackson MC (1993) Cycling of sulfur in subduction zones: the geochemistry of sulfur in the Mariana Island Arc and back-arc trough. Earth Planet Sci Lett 119:477–494

Andersson UB (1997) Petrogenesis of some Proterozoic granitoid suites and associated basic rocks in Sweden (geochemistry and isotope geology). SGU Rapp Medd 91:216

Barker AK, Coogan LA, Gillis KM, Weis D (2008) Strontium isotope constraints on fluid flow in the sheeted dike complex of fast spreading crust: pervasive fluid flow at Pito Deep. Geochem Geophys Geosyst. doi:10.1029/2007GC001901

Barker AK, Holm PM, Peate DW, Baker JA (2009) Geochemical stratigraphy of submarine lavas (3–5 Ma) from the Flamengos Valley, Santiago, Cape Verde. J Petrol 50:169–193. doi:10.1093/petrology/egn081

Barker AK, Holm PM, Peate DW, Baker JA (2010) A five million year record of compositional variations in mantle sources to magmatism on Santiago, southern Cape Verde archipelago. Contrib Mineral Petrol 160:133–154. doi:10.1007/s00410-009-0470-x

Carracedo JC, Day S, Guillou H, Rodríguez Badiola E, Canas JA, Torrado P (1998) Hotspot volcanism close to a passive continental margin: the Canary Islands. Geol Mag 135:591–604. doi:10.1017/S0016756898001447

Chan L-H, Alt JC, Teagle DAH (2002) Lithium and lithium isotope profiles through the upper oceanic crust: a study of seawater-basalt exchange at ODP Sites 504B and 896A. Earth Planet Sci Lett 201:187–201

Courtney RC, White RS (1986) Anomalous heat-flow and geoid across the Cape Verde Rise: evidence for dynamic support from a thermal plume in the mantle. Geophys J R Astron Soc 87:815–867

Crough ST (1978) Thermal origin of mid-plate hot-spot swells. Geophys J R Astron Soc 55:451–469

Davies GR, Norry MJ, Gerlach DC, Cliff RA (1989) A combined chemical and Pb-Sr-Nd isotope study of the Azores and Cape

Verde hot-spots: the geodynamic implications. In: Saunders AD, Norry MJ (Eds) Magmatism in Ocean Basins. Geol Soc Lond Special Publ 42:231–255

de Hoog JCM, Taylor BE, van Bergen MJ (2001) Sulfur isotope systematics of basaltic lavas from Indonesia: implications for the sulfur cycle in subduction zones. Earth Planet Sci Lett 189:237–252

DePaolo DJ, Wasserburg GJ (1979) Petrogenetic mixing models and Nd-Sr isotopic patterns. Geochim Cosmochim Acta 43:15–27

Donoghue E, Troll VR, Harris C, O'Halloran A, Walter TR, Torrado FJP (2008) Low-temperature hydrothermal alteration of intra-caldera tuffs, Miocene Tejeda caldera, Gran Canaria, Canary Islands. J Volcanol Geotherm Res 176:551–564

Doucelance R, Escrig S, Moriera M, Gariepy C, Kurz M (2003) Pb-Sr-He isotope and trace element geochemistry of the Cape Verde Archipelago. Geochimicia et Cosmochimica Acta 67:3717–3733

Dyhr CT, Holm PM (2010) A volcanological and geochemical investigation of Boa Vista, Cape Verde Islands; $^{40}Ar/^{39}Ar$ geochronology and field constraints. J Volcanol Geotherm Res 189:19–32

Eisele J, Abouchami W, Galer SJG, Hofmann AW (2003) The 320 kyr Pb isotope evolution of Mauna Kea lavas recorded in the HSDP-2 drill core. Geochem Geophys Geosyst 4:8710. doi: 10.1029/2002GC000339

Ellam RM (2006) New constraints on the petrogenesis of the Nuanetsi picrite basalts from Pb and Hf isotope data. Earth Planet Sci Lett 245:153–161

Escrig S, Doucelance R, Moreira M, Allégre C (2005) Os isotope systematics in Fogo Island: evidence for lower continental crust fragments under the Cape Verde Southern Islands. Chem Geol 219:93–113

Ewart A, Griffin WL (1994) Application of proton-microprobe data to trace-element partitioning in volcanic rocks. Chem Geol 117:251–284

Fagereng A, Harris C, LaGrange M, Stevens G (2008) Stable isotope study of the Archaen rocks of the Vredefort impact structure, central Kaapvaal Craton, South Africa. Contrib Mineral Petrol 155:63–78

Geist DJ, White WM, McBirney AR (1988) Plume-asthenosphere mixing beneath the Galapagos Archipelago. Nature 333:657–660

Geldmacher J, Hoernle K, Klügel A, van den Bogaard P, Bindeman I (2008) Geochemistry of a new enriched mantle type locality in the northern hemisphere: implications for the origin of the EM-I source. Earth Planet Sci Lett 265:167–182

Gerlach DC, Cliff RA, Davies GR, Norry M, Hodgson N (1988) Magma sources of the Cape Verdes archipelago: isotopic and trace element constraints. Geochimicia et Cosmochimica Acta 52:2979–2992

Grassineau NV, Mattey DP, Lowry D (2001) Sulfur isotope analysis of sulfide and sulfate minerals by continuous flow-isotope ratio mass spectrometry. Anal Chem 73:220–225

Grevemeyer I, Helffrich G, Faria B, Booth-Rea G, Schnabel M, Weinrebe RW (2010) Seismic activity at Cadamosto seamount near Fogo Island, Cape Verdes—formation of a new ocean island? Geophys J Int 180:552–558. doi:10.1111/j.1365-246X.2009.04440.x

Gurenko AA, Chaussidon M, Schmincke H-U (2001) Magma ascent and contamination beneath one intraplate volcano: evidence from S and O isotopes in glass inclusions and their host clinopyroxenes from Miocene basaltic hyaloclastites southwest of Gran Canaria (Canary Islands). Geochim Cosmochim Acta 65:4359–4374

Hansteen T, Troll VR (2003) Oxygen isotope composition of xenoliths from the oceanic crust and volcanic edifice beneath Gran Canaria (Canary Islands): consequences for crustal contamination of ascending magmas. Chem Geol 193:181–193

Harris C, Vogeli J (2010) Oxygen isotope composition of garnet in the peninsula granite, Cape granite suite, South Africa: constraints on melting and emplacement mechanisms. S Afr J Geol 113:385–396

Harris C, Smith HS, le Roex AP (2000) Oxygen isotope composition of phenocrysts from Tristan da Cunha and Gough Island lavas: variation with fractional crystallisation and evidence for assimilation. Contrib Mineral Petrol 138:164–175

Hart SR (1984) A large-scale isotopic anomaly in the southern hemisphere mantle. Nature 309:753–757

Hildner E, Klügel A, Hauff F (2011) Magma storage and ascent during the 1995 eruption of Fogo, Cape Verde archipelago. Contrib Mineral Petrol. doi: 10.1007/s00410-011-0623-6

Hill IA (1985) Geophysical studies of the Cape Verde archipelago. RRS Charles Darwin Cruise Report 8-85. University of Leicester

Hoernle K (1998) Geochemistry of Jurassic oceanic crust beneath Gran Canaria (Canary Islands): implications for crustal recycling and assimilation. J Petrol 39:859–880

Hoernle K, Tilton G, Schminke H-U (1991) Sr-Nd-Pb isotopic evolution of Gran Canaria: evidence for shallow enriched mantle beneath the Canary Islands. Earth Planet Sci Lett 106:44–63

Hoernle K, Werner R, Morgan JP, Garbe-Schönberg D, Bryce J, Mrazek J (2000) Existence of complex spatial zonation in the Galápagos plume for at least 14 m.y. Geology 28:435–438

Holm PM, Wilson JR, Christensen BP, Hansen L, Hansen SL, Hein KH, Mortensen AK, Pedersen R, Plesner S, Runge MK (2006) Sampling the Cape Verde mantle plume: evolution of melt compositions on Santo Antão, Cape Verde Islands. J Petrol 47:145–189

Hubberton HW (1983) Sulfur content and sulfur isotopes of basalts from the Costa Rica Rift (Hole 504B, DSDP Legs 69 and 70). In Initial Reports DSDP (eds J. Honnorez et al.,) 69:629–635. doi: 10.2973/dsdp.proc.69.136.1983

Ito E, White WM, Gopel C (1987) The O, Sr, Nd, and Pb isotope geochemistry of MORB. Chem Geol 62:157–176

Kawahata H, Kusakabe M, Kikuchi Y (1987) Strontium, oxygen, and hydrogen isotope geochemistry of hydrothermally altered and weathered rocks in DSDP Hole 504B, Costa Rica Rift. Earth Planet Sci Lett 85:343–355

Kokfelt TF, Holm PM, Hawkesworth CJ, Peate DW (1998) A lithospheric mantle source for the Cape Verde Island magmatism: trace element and isotopic evidence from the Island of Fogo. Mineral Mag 62A:801–802

Lodge A, Helffrich G (2006) Depleted swell root beneath the Cape Verde Islands. Geology 34:449–452

Madeira J, Mata J, Maurão C, da Silveira AB, Martins S, Ramalho R, Hoffmn DL (2010) Volcano-stratigraphy and structural evolution of Brava Island (Cape Verde) based on $^{40}Ar/^{39}Ar$, U-Th and field constraints. J Volcanol Geotherm Res 196:219–235

Martins S, Mata J, Munhá J, Mendes MH, Maerschalk C, Caldeira R, Mattielli N (2009) Chemical and mineralogical evidence of the occurrence of mantle metasomatism by carbonate-rich melts in an oceanic environment (Santiago Island, Cape Verde). Mineral Petrol. doi: 10.1007/s00710-009-0078-x

Melguen M (1978) Facies evolution, carbonate dissolution cycles in sediments from the eastern south Atlantic (DSDP Leg 40) since the early Cretaceous. Initial Reports DSDP, volume XL, Washington US Government Printing Office

Meyer R, Nicoll GR, Hertogen J, Troll VR, Ellam RM, Emeleus CH (2009) Trace element and isotope constraints on crustal anatexis by upwelling mantle melts in the North Atlantic Igneous province: an example from the Isle of Rum, NW Scotland. Geol Mag 146:382–399

Millet M-A, Doucelance R, Schiano P, David K, Bosq C (2008) Mantle plume heterogeneity versus shallow-level interactions: a case study, the São Nicolau Island, Cape Verde archipelago.

J Volcanol Geotherm Res 176:265–276. doi:10.1016/j.jvolgeores.2008.04.003

Montelli R, Nolet G, Dahlen FA, Masters G, Engdahl ER, Hung S-H (2004) Finite-frequency tomography reveals a variety of plumes in the mantle. Science 30:338–343

Morimoto N, Fabries J, Ferguson AK, Ginzburg IV, Ross M, Siefert FA, Zussman J, Aoki K, Gottardi G (1988) Nomenclature of pyroxenes. Am Mineral 73:1123–1133

O'Hara MJ (1998) Volcanic plumbing and the space problem-thermal and geochemical consequences of large-scale assimilation in ocean island development. J Petrol 39:1077–1089

Pedersen RB, Furnes H (2001) Nd- and Pb-isotopic variations through the upper oceanic crust in DSDP/ODP Hole 504B, Costa Rica Rift. Earth Planet Sci Lett 189:221–235

Pim J, Peirce C, Watts AB, Grevemeyer L, Krabbenhoeft A (2008) Crustal structure and origin of the Cape Verde Rise. Earth Planet Sci Lett 272:422–428

Putirka K (2008) Thermometers and barometers for volcanic systems. Rev Mineral Geochem 69:61–120

Putirka K, Mikaelian H, Ryerson FJ, Shaw H (2003) New clinopyroxene-liquid thermobarometers for mafic, evolved and volatile-bearing lava compositions, with applications to lavas from Tibet and the Snake River Plain, ID. Am Mineral 88:1542–1554

Rees CE, Jenkins WJ, Monster J (1978) The sulphur isotopic composition of ocean water sulphate. Geochim Cosmochim Acta 42:377–381

Regelous M, Hofmann AW, Abouchami W, Galer SJG (2003) Geochemistry of lavas from the Emperor Seamounts, and the geochemical evolution of Hawaiian magmatism from 85 to 42 Ma. J Petrol 44:113–140

Sakai H, Casadevall TJ, Moore JG (1982) Chemistry and isotope ratios of sulfur in basalts and volcanic gases at Kilauea Volcano, Hawaii. Geochim Cosmochim Acta 46:729–738

Sakai H, Des Marias DJ, Ueda A, Moore JG (1984) Concentrations and isotope ratios of carbon, nitrogen and sulfur in ocean-floor basalts. Geochim Cosmochim Acta 48:2433–2441

Shanks WC III, Bischoff JL, Rosenbauer RJ (1981) Seawater sulfate reduction and sulfur isotope fractionation in basaltic systems: interaction of seawater with fayalite and magnetite at 200–350°C. Geochim Cosmochim Acta 45:1977–1995

Spera FJ, Bohrson WA (2001) Energy-constrained open-system magmatic processes I: general model and energy-constrained assimilation and fractional crystallisation (EC-AFC) formulation. J Petrol 42:999–1018

Taylor HP Jr, Sheppard SMF (1986) Igneous Rocks 1. Processes of isotopic fractionation and isotope systematics. In: Valley JW, Taylor HP Jr, and O'Neil JR (Eds) Stable isotopes in high temperature geological processes. Rev Mineral 16:227–271

Thirlwall MF, Gee MAM, Taylor RN, Murton BJ (2004) Mantle components in Iceland and adjacent ridges investigated using double-spike Pb isotope ratios. Geochim Cosmochim Acta 68:361–386

Tiepolo M, Oberti R, Vannucci R (2002) Trace-element incorporation in titanite: constraints from experimentally determined solid/liquid partition coefficients. Chem Geol 191:105–119

Ueda A, Sakai H (1984) Sulfur isotope study of Quaternary volcanic rocks from the Japanese Islands Arc. Geochim Cosmochim Acta 48:1837–1848

Venneman TW, Smith HS (1990) The rate and temperature of reaction of ClF_3 with silicate minerals, and their relevance to oxygen isotope analysis. Chem Geol (Isotope Geosci Sect) 86:83–88

Von Damm KL (2000) Chemistry of hydrothermal vent fluids from 9–10°N, East Pacific Rise: "Time zero", the immediate posteruptive period. J Geophys Res 105:11203–11222

Wallace P, Carmichael ISE (1992) Sulfur in basaltic magmas. Geochim Cosmochim Acta 56:1863–1874

Weaver BL (1990) Geochemistry of highly-undersaturated ocean island basalt suites from the South Atlantic Ocean: Fernando de Noronha and Trindade islands. Contrib Mineral Petrol 105:502–515

Zhao Z-F, Zheng Y-F (2003) Calculation of oxygen isotope fractionation in magmatic rocks. Chem Geol 193:59–80